

## Synchronization of a Silica Microcomb to a Mode-locked Laser with a Fractional Optoelectronic Phase-locked Loop

Hui Yang<sup>1,2†</sup>, Changmin Ahn<sup>1†</sup>, Igju Jeon<sup>1</sup>, Daewon Suk<sup>1</sup>, Hansuek Lee<sup>1</sup>, and Jungwon Kim<sup>1\*</sup>

<sup>1</sup>Korea Advanced Institute of Science and Technology (KAIST), Daejeon 34141, Korea

<sup>2</sup>School of Information Science and Technology, Southwest Jiaotong University, Chengdu 610031, China

(Received May 2, 2023 : revised July 14, 2023 : accepted July 24, 2023)

Ultralow-noise soliton pulse generation over a wider Fourier frequency range is highly desirable for many high-precision applications. Here, we realize a low-phase-noise soliton pulse generation by transferring the low phase noise of a mode-locked laser to a silica microcomb. A 21.956-GHz and a 9.9167-GHz Kerr soliton combs are synchronized to a 2-GHz and a 2.5-GHz mode-locked laser through a fractional optoelectronic phase-locked loop, respectively. The phase noise of the microcomb was suppressed by up to ~40 dB at 1-Hz Fourier frequency. This result provides a simple method for low-phase-noise soliton pulse generation, thereby facilitating extensive applications.

**Keywords** : Fractional optoelectronic phase-locked loop, Microcomb, Mode-locked lasers, Stability transfer, Synchronization

**OCIS codes** : (140.3945) Microcavities; (140.4050) Mode-locked lasers; (320.7160) Ultrafast technology

### I. INTRODUCTION

An optical frequency comb (OFC) can provide a series of frequency components with a certain phase relationship on the spectrum and bring revolutionary changes in a wide range of applications in the last two decades [1]. Mode-locked laser (MLL)-based OFC has facilitated various high-timing-precision applications owing to its low jitter characteristic [2–8]. However, to realize repetition rates of tens of gigahertz using MLL-based combs remain challenging owing to its intrinsically narrow comb-line spacing. Microresonator-based OFCs (microcombs) have garnered significant attention owing to the ability to provide high repetition rates from ~10 GHz to ~1 THz with compact size. This is highly desirable for applications such as microwave generation [9, 10], high-speed telecommunications [11, 12] and astronomical spectrometer calibration [13], to name a few. Although the potential for ultra-low timing jit-

ter and phase noise has been demonstrated by free-running microcombs [14–16], it is desirable to suppress the phase noise over a wider range of Fourier frequencies as well as time scales to satisfy future high precision requirements. However, it is often challenging to lock a microcomb to a more stable source due to the very limited locking range of the microcombs.

In this paper, a simple method to improve the low-offset-frequency phase noise of microcombs is proposed through synchronization to an MLL-based OFC with a fractional optoelectronic phase-locked loop (PLL), which can transfer the frequency stability of the MLL to the microcomb. Here, the fractional optoelectronic PLL comprises an electro-optic sampling-based timing detector (EOS-TD) [17, 18] and an external microwave source. In general, the input optical frequency and input microwave signal frequency of the EOS-TD must satisfy a harmonic relationship, which limits the practical applications of optical combs with a

<sup>†</sup>These authors contributed equally to this paper.

\*Corresponding author: jungwon.kim@kaist.ac.kr, ORCID 0000-0001-5979-5774

Color versions of one or more of the figures in this paper are available online.



This is an Open Access article distributed under the terms of the Creative Commons Attribution Non-Commercial License (<http://creativecommons.org/licenses/by-nc/4.0/>) which permits unrestricted non-commercial use, distribution, and reproduction in any medium, provided the original work is properly cited.

Copyright © 2023 Current Optics and Photonics

narrow tuning range. To overcome this limitation, an external microwave source, which can be either a direct digital synthesizer (DDS) or a signal generator, is used to down-convert the frequency error signal, which facilitates a fractional frequency division factor. As a proof-of-concept experiment, a 21.956-GHz (9.9167-GHz) dissipative Kerr soliton silica microcomb was synchronized to a 2.000-GHz (2.500-GHz) MLL with an EOS-TD-based fractional PLL method. For the 21.956-GHz microcomb, the phase noise after synchronization was improved by more than 40 dB (25 dB) at 1-Hz (100-Hz) Fourier frequency and for the 9.9167-GHz microcomb, the phase noise was suppressed by more than 30 dB (15 dB) at 1-Hz (100-Hz) Fourier frequency. These results indicate the feasibility of adopting the stable transmission mode for the microcomb. Owing to its stability and low operational complexity, it is advantageous for a variety of application scenarios, including radio astronomy, photonics-based radars, high-speed telecommunications, and signal analysis instruments.

## II. EXPERIMENT SETUP

The experimental setup employed to synchronize the silica microcomb to the MLL-based OFC is shown in Fig. 1(a). It includes a 2-GHz (2.5-GHz) MLL oscillator (Menhir Photonics) as the master oscillator, a silica microcomb with a free spectral range ( $D/2\pi$ ) of 21.956-GHz (9.9167-GHz) as the slave oscillator, and an EOS-TD as the phase detector.

The central component for achieving the stability transfer is the EOS-TD. Figure 1(b) shows a schematic diagram of the EOS-TD [17, 18], which is a well-established technique that can synchronize the microwave signal to the optical pulse train or vice versa. Its key component is the polarization-maintaining fiber Sagnac loop, which consists of a unidirectional high-speed LiNbO<sub>3</sub> phase modulator and a non-reciprocal phase bias unit. The optical pulse passes through

a circulator and a 3-dB coupler, and is transmitted along the clockwise and counterclockwise directions of the Sagnac loop. The two outputs ( $P_1 = P_{in}\cos^2(\Delta\phi/2)$ ,  $P_2 = P_{in}\sin^2(\Delta\phi/2)$ , where  $P_{in}$  represents the input optical power and  $\Delta\phi$  represents the optical phase difference between counterpropagating pulses in the loop) interfere with each other at the 3-dB coupler. A nonreciprocal bias introduces an additional  $\pi/2$  phase difference between counter-propagating pulses in the fiber loop. The phase modulator is modulated by a microwave signal with a frequency of integer-multiple to the optical pulse. The timing difference  $\tau_e$  between optical pulses and microwave signals is mapped to the amplitude imbalance between the two Sagnac loop outputs. When detected by a balanced photodetector (BPD), the output voltage signal can be represented as  $V_e = GRP_{avg} \sin[\varphi_0 \sin(\tau_e)]$ , where  $G$  and  $R$  represent the transimpedance gain and responsivity of the BPD, respectively,  $P_{avg}$  is the average optical power of the two Sagnac loop outputs, and  $\varphi_0$  is the modulation depth of the phase modulator. When the zero-crossings of the microwave signal are aligned with the optical pulses, *i.e.*  $\tau_e = 0$ , the output voltage of the BPD is also 0. When  $\tau_e \neq 0$ ,  $V_e$  has an approximately linear relationship with  $\tau_e$ ,  $V_e \approx GRP_{avg} \varphi_0 \tau_e$ , which can be used for precise optical-microwave timing detection.

The silica wedge resonator has been described previously in [9, 19]. To generate a stable coherent Kerr soliton, first, a narrow linewidth CW laser (at 1,550 nm) was amplified by an Er-doped fiber amplifier (EDFA) to  $\sim 500$  mW. Then it is passed through an acousto-optic frequency shifter (AOFS), which is driven by a voltage-controlled oscillator (VCO). An arbitrary waveform generator (AWG) that dictates the speed and range of the laser's frequency sweep on the microresonator was used to apply voltage to the VCO. The output of the AOFS then passed through a polarization controller before being injected into a silica wedge microresonator using a tapered fiber. Power kicking and active

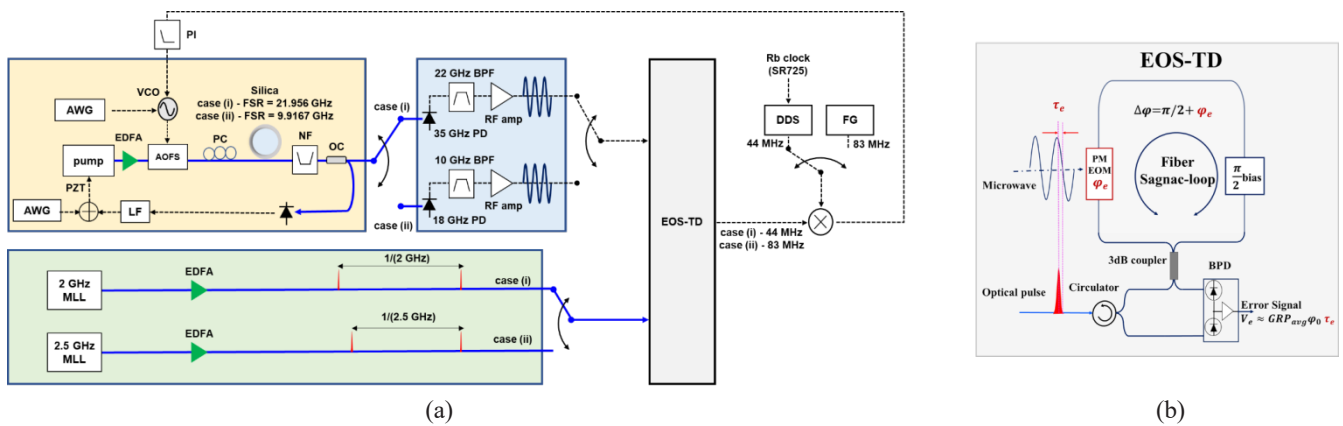


**FIG. 1.** Experimental setup. (a) Schematic of synchronization of a silica microcomb to a mode-locked laser with EOS-TD. (b) Schematic diagram of electro-optic sampling-based timing detector (EOS-TD). AWG, arbitrary waveform generator; AOFS, acousto-optic frequency shifter; EDFA, Er-doped fiber amplifier; PC, polarization controller; NF, notch filter; OC, optical coupler; PD, photodetector; VCO, voltage-controlled oscillator; PI, proportional-integral servo controller; BPF, bandpass filter; AMP, amplifier; DDS, direct digital synthesizers; PZT, piezoelectric transducer; LPF, lowpass filter; EOM, travelling-wave electro-optic phase modulator; BPD, balanced photodetector; FG, function generator.

capture were adopted to lock the soliton mode [20, 21]. The piezoelectric transducer (PZT) of the pump laser locked the detuning of the pump cavity to prevent the thermal imbalance of the soliton, and fast power modulation in a few microseconds and frequency modulation was implemented upon the generation of a soliton. Furthermore, a notch filter (NF) capable of removing the residual optical pump was used to filter it from the output of the microresonator. We can see the optical spectrum of the generated solitons in Fig. 2. Optical couplers can split an optical signal into two distinct parts, wherein, 10% is applied for the feedback control to the pump, while the remaining 90% is amplified and applied to a modified uni-travelling carrier (MUTC) photodiode or a *p-i-n* photodiode to generate microwaves.

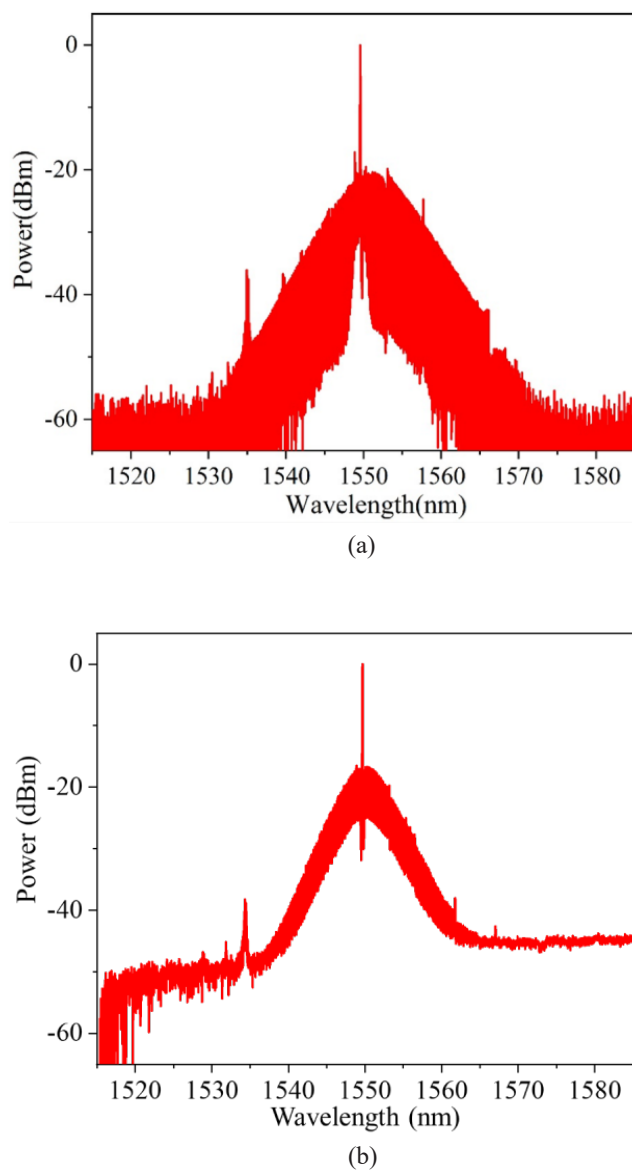


**FIG. 2.** The output optical spectrum of the silica microcomb used (a) with a 21.956-GHz repetition rate and (b) 9.9167 GHz repetition rate.

Bandpass filters centered at 22-GHz and 10-GHz were used to filter the generated microwaves at 21.956 GHz and 9.9167 GHz, followed by a low phase noise RF amplifier with a maximum value of +10 dBm to amplify for phase detection.

In each case, the MLL outputs 2-GHz and 2.5-GHz repetition rate reference light. The output optical signal was amplified by an EDFA, and then entered the EOS-TD for timing detection.

Usually, the frequency of the microwave source signal used needs to be an integer multiple of the repetition frequency of the optical pulse. However, due to the very limited locking range of the microcomb, it is challenging to lock a microcomb to a stable MLL. In this work, by fully utilizing the EOS-TD and an external microwave source, which can be either a DDS or signal generator, we showed a way to transfer the stability of the MLL to the microcomb even when their repetition rate is not a harmonic relationship. Since the microwave frequency [21.956-GHz for case (i) and 9.9167-GHz for case (ii)] is not an integer-multiple of the mode-locked laser repetition rate [2 GHz for case (i) and 2.5 GHz for case (ii)], a 44-MHz microwave from a DDS, which was locked to an Rb clock [for case (i)] or a 83-MHz microwave from signal generator [for case (ii)] was mixed with the EOS-TD output to convert the error signal to  $\sim$ kHz with an ultralow phase noise. The output represents the relative phase error between the optical pulse and the zero-crossing point of the microwave signal. With the feedback control of the pump frequency modulation enabled by the VCO frequency modulation, the high-precision synchronization between the MLL and microwave source can be achieved, stabilizing the microcomb to the MLL when the control loop is activated.

### III. RESULTS

To test the effectiveness of system, systems with and without synchronization were compared for case (i). The phase noise of the generated 21.956 GHz signal is shown in Fig. 3. At 1-Hz offset frequency, more than 40 dB of phase noise is suppressed. At the 100-Hz offset frequency, the free-running phase noise of the microcomb was  $-19$  dBc/Hz without finding a quiet point. Here, the peaks at 20 kHz and 60 kHz are the resonance peak of the control loop for active capturing of the soliton state and the peak from the soliton RIN-coupled jitter [19], respectively. After the control loop was activated, the phase noise reached  $-45$  dBc/Hz at 100-Hz offset frequency. The transfer method offered an improvement  $>25$  dB compared to the free-running Kerr comb, thus exhibiting an ability to improve the frequency stability of microcombs. Furthermore, the phase noise was below  $-90$  dBc/Hz at 10-kHz and  $-140$  dBc/Hz at approximately 1 MHz, demonstrating that the low noise properties of soliton Kerr combs were not lost at high Fourier frequencies.

For case (ii), performance of the system was analyzed by measuring the phase noise of the free-running and synchronized microcomb and the residual phase noise of the

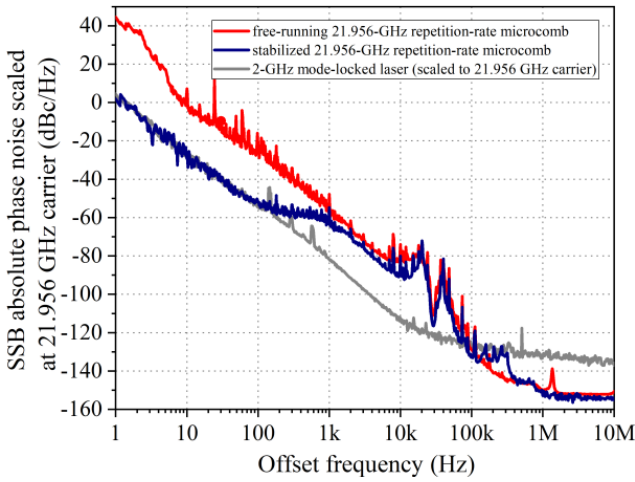


**FIG. 3.** The absolute single sideband (SSB) phase noise of the generated Kerr comb.

control loop [Fig. 4(a)]. The phase noise of the microcomb was measured with a phase noise analyzer. The out-of-loop (OOL) EOS-TD was implemented to characterize the residual phase noise. The voltage power spectral density of the down-converted OOL EOS-TD output was measured by fast Fourier transform analyzer and converted to the residual phase noise by dividing it by detection sensitivity. Here, an additional manual delay line was inserted in the OOL path to adjust the down-converted OOL EOS-TD output to the zero-crossing so that minimization of the intensity noise effect as well as maximization of the detection sensitivity could be achieved.

The measurement result is shown in Fig. 4(b). For the free-running microcomb, the absolute phase noise was  $-20$  dBc/Hz ( $-54$  dBc/Hz) at 10 Hz (100 Hz) offset frequency. When the microcomb was synchronized, the phase noise was well suppressed to  $-33$  dBc/Hz ( $-70$  dBc/Hz) at 10 Hz (100 Hz) offset frequency. In the residual phase noise, it was clearly seen that the control bandwidth, which was limited by the loop filter cutoff frequency, was 1 kHz. The limited control bandwidth could be attributed to the repetition rate tuning actuator. Since the residual phase noise was lower than the absolute phase noise of the mode-locked laser at offset frequencies below 200 Hz, the phase noise of the synchronized microcomb followed that of the mode-locked laser. On the other hand, since the residual phase noise was larger than the absolute phase noise of the mode-locked laser at higher offset frequencies, the phase noise of the synchronized microcomb followed that of the residual phase noise, which eventually followed the phase noise of the free-running case. It should be noted that we did not actively find the quiet point condition, but rather used a relatively high noise condition of the microcomb in this work.

#### IV. CONCLUSION

This study proposed a simple method to obtain high fre-

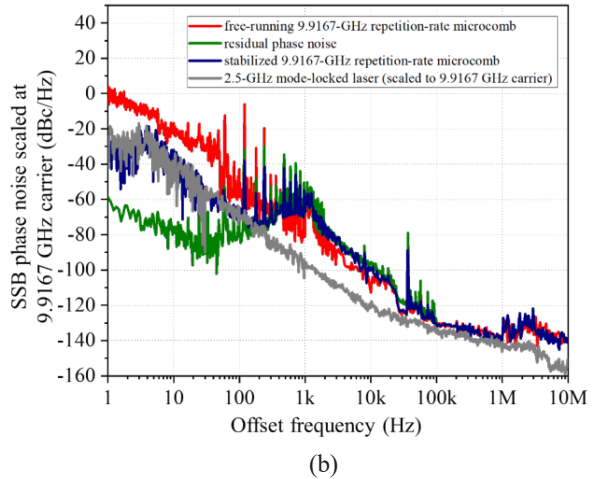
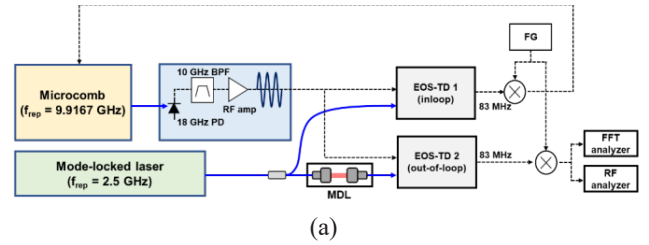


**FIG. 4.** Phase noise data. (a) The experimental setup for residual phase noise measurement and (b) the measurement result. PD, photodetector; RF amp, RF amplifier; MDL, manual delay line;  $f_{\text{rep}}$ , repetition rate; EOS-TD, electro-optic sampling-based timing detector; FG, function generator; PD, photodetector; FFT analyzer, fast Fourier transform analyzer.

quency stability microcombs by transferring the stability from an MLL, which is desirable for scenarios requiring a high repetition rate, high stability, and easy operation. Here, its applicability to various situations was shown by demonstrating two different combinations of the microcomb and the mode-locked laser. The 21.956-GHz (9.9167-GHz) Kerr solitons were generated using this method with single sideband (SSB) phase noise of  $-45$  dBc/Hz ( $-70$  dBc/Hz) at 100-Hz offset frequency, which is  $>25$  dB ( $>15$  dB) suppression compared to the free-running condition. The phase noise of the stabilized microcomb follows the converted phase noise of the 2-GHz (2.5 GHz) MLL up to  $\sim 130$  Hz ( $\sim 200$  Hz) offset frequency. These experimental results reveal that the proposed method can improve the phase noise of the microcomb at low offset frequency and long-term frequency stability, while preserving the free-running phase noise at high offset frequency. In particular, one does not need an exact harmonic relationship between an MLL and a microcomb to achieve the stability transfer, which makes it very suitable for stabilizing a microcomb with a small tuning range. Note that the minimum frequency difference between the repetition rate of the microcomb and the integer multiples of the repetition rate of the mode-locked laser is expected to be tens of kHz considering the cutoff frequency of the mixer and the control bandwidth

of the synchronization loop. It is believed that the proposed MLL-to-microcomb frequency stability transfer method holds promising potential for a wider range of scenarios requiring ultralow noise and high repetition rate applications.

## FUNDING

National Research Council of Science and Technology (NST) of Korea (CAP22061-000).

## ACKNOWLEDGMENTS

H. Yang thanks the China Scholarship Council and State Key Laboratory of Advanced Optical Communication Systems Networks, China, for support in performing the visiting research at KAIST, Republic of Korea.

## DISCLOSURES

The authors declare that they have no known competing financial interests or personal relationships that could have appeared to influence the work reported in this paper.

## DATA AVAILABILITY

Data underlying the results presented in this paper are not publicly available at the time of publication, but may be obtained from the authors upon reasonable request.

## REFERENCES

1. T. Fortier and E. Baumann, "20 years of developments in optical frequency comb technology and applications," *Commun. Phys.* **2**, 153 (2019).
2. T. Udem, J. Reichert, R. Holzwarth, and T. Hänsch, "Absolute optical frequency measurement of the cesium D1 line with a mode-locked laser," *Phys. Rev. Lett.* **82**, 3568–3571 (1999).
3. P. J. Delfyett, S. Gee, M. T. Choi, H. Izadpanah, W. Lee, S. Ozharar, F. Quinlan, and T. Yilmaz, "Optical frequency combs from semiconductor lasers and applications in ultrawideband signal processing and communications," *J. Lightwave Technol.* **24**, 2701–2719 (2006).
4. Y. Na, C. G. Jeon, C. Ahn, M. Hyun, D. Kwon, J. Shin, and J. Kim, "Ultrafast, sub-nanometre-precision and multifunctional time-of-flight detection," *Nat. Photonics* **14**, 355–360 (2020).
5. X. Xie, R. Bouchand, D. Nicolodi, M. Giunta, W. Hänsel, M. Lezius, A. Joshi, S. Datta, C. Alexandre, M. Lours, P. A. Tremblin, G. Santarelli, R. Holzwarth, and Y. L. Coq, "Photonic microwave signals with zeptosecond-level absolute timing noise," *Nat. Photonics* **11**, 44–47 (2017).
6. J. Kim, J. A. Cox, J. Chen, and F. X. Kärtner, "Drift-free femtosecond timing synchronization of remote optical and microwave sources," *Nat. Photonics* **2**, 733–736 (2008).
7. I. Coddington, W. C. Swann, L. Nenadovic, and N. R. Newbury, "Rapid and precise absolute distance measurements at long range," *Nat. Photonics* **3**, 351–356 (2009).
8. S. Schulz, I. Grguras, C. Behrens, H. Bromberger, J. T. Costello, M. K. Czwalińska, M. Felber, M. C. Hoffmann, M. Ilchen, H. Y. Liu, T. Mazza, M. Meyer, S. Pfeiffer, P. Prędki, S. Schefer, C. Schmidt, U. Wegner, H. Schlarb, and A. L. Cavalieri, "Femtosecond all-optical synchronization of an X-ray free-electron laser," *Nat. Commun.* **6**, 5938 (2015).
9. D. Kwon, D. Jeong, I. Jeon, H. Lee, and J. Kim, "Ultrastable microwave and soliton-pulse generation from fibre-photonic-stabilized microcombs," *Nat. Commun.* **13**, 381 (2022).
10. E. Lucas, P. Brochard, R. Bouchand, S. Schilt, T. Südmeyer, and T. J. Kippenberg, "Ultralow-noise photonic microwave synthesis using a soliton microcomb-based transfer oscillator," *Nat. Commun.* **11**, 374 (2020).
11. Y. Geng, H. Zhou, X. Han, W. Cui, Q. Zhang, B. Liu, G. Deng, Q. Zhou, and K. Qiu, "Coherent optical communications using coherence-cloned Kerr soliton microcombs," *Nat. Commun.* **13**, 1070 (2022).
12. S. Fujii, S. Tanaka, T. Ohtsuka, S. Kogure, K. Wada, H. Kumazaki, S. Tasaka, Y. Hashimoto, Y. Kobayashi, T. Araki, K. Furusawa, N. Sekine, S. Kawanishi, and T. Tanabe, "Dissipative Kerr soliton microcombs for FEC-free optical communications over 100 channels," *Opt. Express* **30**, 1351–1364 (2022).
13. M.-G. Suh, X. Yi, Y.-H. Lai, S. Leifer, I. S. Grudinin, G. Vasisht, E. C. Martin, M. P. Fitzgerald, G. Doppmann, J. Wang, D. Mawet, S. B. Papp, S. A. Diddams, C. Beichman, and K. Vahala, "Searching for exoplanets using a microresonator astroc comb," *Nat. Photonics* **13**, 25–30 (2019).
14. W. Weng, E. Lucas, G. Lihachev, V. E. Lobanov, H. Guo, M. L. Gorodetsky, and T. J. Kippenberg, "Spectral purification of microwave signals with disciplined dissipative Kerr solitons," *Phys. Rev. Lett.* **122**, 013902 (2019).
15. J. Liu, E. Lucas, A. S. Raja, J. He, J. Riemensberger, R. N. Wang, M. Karpov, H. Guo, R. Bouchand, and T. J. Kippenberg, "Photonic microwave generation in the X- and K-band using integrated soliton microcombs," *Nat. Photonics* **14**, 486–491 (2020).
16. Y. Bai, M. Zhang, Q. Shi, S. Ding, Y. Qin, Z. Xie, X. Jiang, and M. Xiao, "Brillouin-Kerr soliton frequency combs in an optical microresonator," *Phys. Rev. Lett.* **126**, 063901 (2021).
17. K. Jung and J. Kim, "Subfemtosecond synchronization of microwave oscillators with mode-locked Er-fiber lasers," *Opt. Lett.* **37**, 2958–2960 (2012).
18. C. Ahn, Y. Na, M. Hyun, J. Bae, and J. Kim, "Synchronization of an optical frequency comb and a microwave oscillator with 53 zs/Hz<sup>1/2</sup> resolution and 10<sup>-20</sup>-level stability," *Photonics Res.* **10**, 365–372 (2022).
19. D. Jeong, D. Kwon, I. Jeon, I. H. Do, J. Kim, and H. Lee, "Ultralow jitter silica microcomb," *Optica* **7**, 1108–1111 (2020).
20. X. Yi, Q.-F. Yang, K. Y. Yang, and K. Vahala, "Active capture and stabilization of temporal solitons in microresonators," *Opt. Lett.* **41**, 2037–2040 (2016).
21. T. Herr, V. Brasch, J. D. Jost, C. Y. Wang, N. M. Kondratiev, M. L. Gorodetsky, and T. J. Kippenberg, "Temporal solitons in optical microresonators," *Nat. Photonics* **8**, 145–152 (2014).